ISBN: 978-3-95450-241-7 ISSN: 2673-5350 doi:10.18429/JACoW-IBIC2022-WE2I3

ADAPTIVE FEEDFORWARD CONTROL OF CLOSED ORBIT DISTORTION CAUSED BY FAST HELICITY-SWITCHING UNDULATORS

M. Masaki†, S. Takano[1], T. Watanabe[1], T. Fujita, H. Dewa, T. Sugimoto[1], M. Takeuchi
JASRI, Hyogo, Japan
H. Maesaka[2], K. Soutome, T. Fukui, H. Tanaka, RIKEN SPring-8 Center, Hyogo, Japan
K. Kubota, SPring-8 Service Co. Ltd., Hyogo, Japan
[1]also at RIKEN SPring-8 Center, Hyogo, Japan
[2]also at JASRI, Hyogo, Japan

Abstract

We developed a new correction algorithm for closed orbit distortion (COD) based on adaptive feedforward control (AFC). The AFC system integrated into the SPring-8 storage ring has proved to be effective in suppressing the fast COD with repetitive patterns caused by helicity-switching undulators. The scheme aims to counteract error sources by feedforward correctors at the position or in the vicinity of error sources to avoid a potential risk of unwanted local orbit bumps, which is known to exist for the global orbit feedback. The new option, AFC, is especially advantageous when an error source causes an angular fluctuation of photon beams such as a fast orbit distortion near undulators. The AFC provides a complementary capability to a so-called fast global orbit feedback (FOFB) for coming next-generation light sources where ultimate light source stability is essentially demanded.

INTRODUCTION

Storage-ring-based light sources have been become essential facilities for photon sciences and related applications including industrial purposes. One of the key advantages for light source users is the brightness of light, which is also related to the degree of transverse coherence. However, high photon beam stability is also essential for successful developments, along with high brightness. In modern or future light sources, the pointing stability of photon beam should be sufficiently smaller than the electron beam size to achieve the inherent light source performance. Beam orbit disturbances in a storage ring can be caused by a variety of error sources. For examples, (i) mechanical motions of magnets or vacuum chambers due to ground motion, cooling water, (ii) electro-magnetic noise of magnet power supplies or RF sources, (iii) magnet pole gap or phase motions, polarization switching kickers of insertion devices (IDs). These disturbances can be suppressed by orbit feedback and feedforward controls, or elimination of the error source itself. In the case that the error sources are unknown, slow or fast global orbit feedback can be an effective countermeasure. On the other hand, when the error sources are known, an ideal solution is to remove the error source itself, but not feasible for all sources. For an example, in the case of ID-derived orbit disturbance due to gap motion or fast switching kicker, feedforward corrections are often used without removing the error sources. The feedforward counter kicks in the vicinity of the error kicks are very effective.

In the SPring-8 storage ring, two twin-helical undulators (THUs) with fast kicker systems: ID23 and ID25 [1, 2] were installed for periodic photon helicity switching in X-ray magnetic circular dichroism experiments at beamlines. Orbit variations due to periodic excitation of the kicker magnets on demand from user experiments have been observed for years, even though ID23 and ID25 are equipped with fast corrector magnets for feedforward corrections to suppress them. The periodic orbit fluctuations, which are synchronized with the kicker excitation, gradually grew up to 10 μm (RMS) or more because of the deterioration with time of feedforward correction accuracy.

To address this issue, based on a fundamental orbit correction strategy to directly counteract an error source to be corrected, we have taken the following points into consideration: (i) the error sources are identified at the two THUs, (ii) the feedforward correction is already equipped, and (iii) the degradation rate of the correction accuracy is slow. We have introduced, instead of a conventional fast global orbit feedback, a new COD correction algorithm based on adaptive feedforward control (AFC) [3], in which the feedforward tables are dynamically updated. The COD variations originating in the two error sources (ID23 and ID25) are independently suppressed by the new AFC system. Our goal for the orbit stabilization is to suppress the COD fluctuations of less than 1 μm RMS during the kicker excitation in a transparent manner where experimental users cannot observe any periodic disturbance.

HELICITY-SWITCHING UNDULATORS OF SPRING-8

Schematics of the THU installed in the SPring-8 storage ring are illustrated in Fig. 1. The twin helical switching system consists of the two helical undulators for right- and left-handed circular polarizations, placed on the upstream and downstream sides, respectively. Five kicker magnets make the dynamical horizontal orbit bumps (orbit A and B as shown in Fig. 1) alternately, for periodic optical helicity switching. The switching-frequency for ID23 is 1 Hz; ID25 can be switched at either 1 or 0.1 Hz. When the electron beam orbit is switched to the orbit A, the radiation from the upstream undulator propagates horizontally off-axis and is

† masaki@spring8.or.jp

ISBN: 978-3-95450-241-7 ISSN: 2673-5350 doi:10.18429/JACoW-IBIC2022-WE2I3

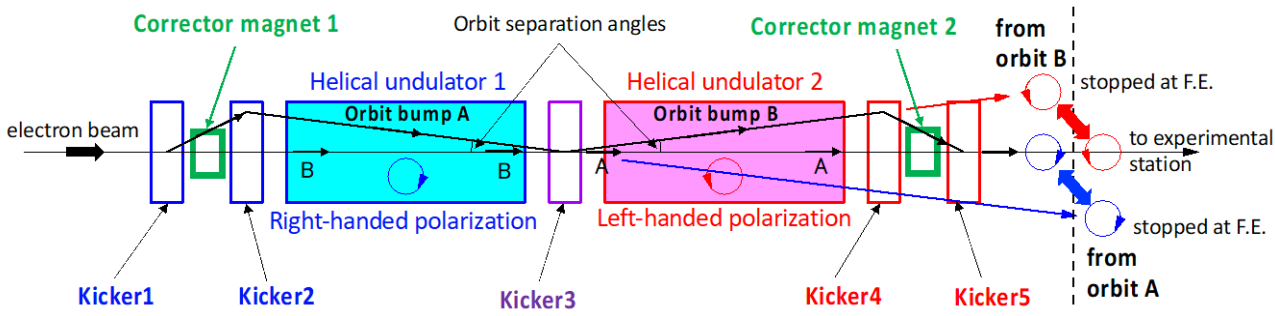

Figure 1: Schematic top view of the twin-helical undulator of SPring-8 with the horizontal kicker system for helicity switching. The orbit separation angles are 300 μrad and 100 μrad for ID23 and ID25, respectively.

stopped at the front-end absorber in the beamline, whereas the radiation from the downstream undulator propagates along the beamline axis and reaches the experimental station. On the other hand, switching to the orbit B makes revered situation. Thus, by switching these two orbits (A and B) repeatedly, the circularly polarized light with alternate helicities is provided for the user's experiments. The photon beam separation angle by the orbits A and B is 300 μrad for ID23 and 100 μrad for ID25. The five kicker magnets are excited with periodic trapezoidal patterns. As a typical example, the excitation pattern of ID23 kickers with a repetition frequency of 1 Hz is shown in Fig. 2. The kickers 1,2,3 to make the orbit bump A are excited in the time range from 0 s to 0.5 s, whereas the kickers 3,4,5 to make the orbit bump B are excited from 0.5 s to 1s.

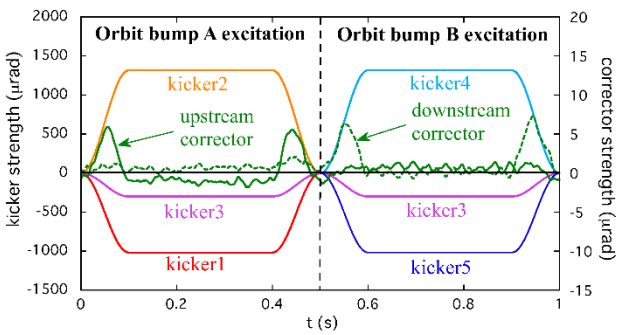

Figure 2: Kicker excitation patterns and examples of excitation patterns for corrector magnets of ID23 for switching at 1 Hz.

The imperfect closure of orbit bumps due to the kicker errors in the THU is supposed to be cancelled out by the feedforward control of two fast air-core corrector magnets placed on both ends of the THU. The waveform-pattern signals to drive the power supplies for the kicker magnets and the fast corrector magnets are generated by a pattern board on a VME system which is prepared for each of ID23 and ID25, separately. The pattern board is equipped with 16 bits D/A converters and outputs the waveform-pattern data sampled synchronously with an internal clock. The clock rate is set to 5 kHz or 1 kHz for the kicker switching frequency of 1 Hz or 0.1 Hz, respectively. While driving the kickers and the fast corrector magnets at 1 Hz or 0.1 Hz, the pattern board also provides the trigger signal outputs synchronized with the kicker pattern excitation.

The feedforward correction tables of fast corrector magnets used to be updated a few times a year. However, as the correction accuracy gradually degraded with time, we sometimes observed periodic orbit fluctuations in the horizontal plane, typically of several microns during the helicity switching, which was detrimental to user experiments. The causes of this deterioration remain unclear, despite having been painstakingly investigated by the Insertion Device Group. This led to the need for an adaptive feedforward system that can dynamically and automatically update the correction tables without stopping the demanded helicity switching in user experiments.

ADAPTIVE FEEDFORWARD CONTROL

We overview the AFC system for helicity-switching undulators developed at SPring-8 [3] by focusing on its specific features and summarizing results from the beam test and operation experiences in the user time.

Key Points of the AFC

In order to mitigate the problem of the periodic orbit perturbation during the optical helicity switching, we have developed the AFC system, which is equipped with dedicated fast BPMs with sufficient time response to detect the orbit variations precisely. The following points are important for the AFC to work effectively: (1) Automatic updating of the correction tables without stopping the helicity switching for user experiments, (2) High-precision and efficient extraction of only error kicks due to the THUs, (3) Even if simultaneous helicity-switching of the two THUs, well-resolving each counter kick, (4) Resistant to orbit perturbations due to error sources other than the THUs.

Correction Scheme

Periodic COD fluctuation occurred in the horizontal plane synchronized to the kickers' driving frequency of 1 or 0.1 Hz during the switching at the two THUs. The observed periodic fluctuation contains frequency components up to several tens of Hz, but these are sufficiently slow compared to the radiation damping time of millisecond order. Therefore, we considered that the orbit distortion at each moment in the switching period can be analyzed as a superposition of instantaneous CODs caused by time-dependent multiple error kicks at the kickers.

ISBN: 978-3-95450-241-7 ISSN: 2673-5350 doi:10.18429/JACoW-IBIC2022-WE2I3

As shown in Fig. 1, each of the orbit bumps A and B is produced by exciting three kickers in a THU. Since the imperfect closure of the three-kicker orbit bump has two error kicks, the leakage of COD variation outside the THU can be suppressed by adding two counter-kicks by exciting the two corrector magnets placed beside the kicker magnets in each THU. The betatron phase difference between the two THUs, ID23 and ID25, is approximately 660° in the horizontal direction, around the ideal value (i.e., an odd multiple of 90°) for resolving the error sources relevant to each THU by observing the distribution of orbit distortion along the storage ring. Therefore, we decided to determine the values for the counter-kicks of the corrector magnets in the two THUs by measuring the orbit variation with multiple BPMs placed along the storage ring. The four counter-kicks for the two THUs can be approximately determined with the data of orbit distortion obtained at four BPMs placed on the ring by solving,

$$-x_{BPM,i}(t) = \sum_{j=1}^{n} R_{ij}\theta_{corr,j}(t)\,, \qquad (1)$$

where $\theta_{corr,j}(t)$ and $x_i(t)$ are the time-dependent counter kick angle at the j-th corrector magnet and the observed beam position displacement at the i-th BPM, respectively. The response-matrix element between the kicker and BPM is

$$R_{ij} \equiv \frac{\sqrt{\beta_i\beta_j}}{2\sin(\pi\nu)}\cos\left(\pi\nu - |\mu_i - \mu_j|\right), \qquad (2)$$

where the parameters β_i, β_j are beta functions at the i-th BPMs and the j-th kickers; ν is the betatron tune; and μ_i-μ_j is the betatron phase advance between the kicker and the BPM, respectively.

System Overview

Figure 3 shows an overview of the AFC system at SPring-8. To resolve the four counter kicks of the corrector magnets even while the two THUs are switching the helicity at the same frequency, we carefully selected four out of the total 286 BPM heads on the storage ring. Each of the selected BPM heads is connected to a newly developed fast MTCA.4-based readout circuit [4] to detect the periodic COD variations with sufficient precisions. We selected two BPMs (namely, 23-2 and 46-2) sensitive to horizontal kicks in ID23, and two others (24-5 and 35-2) for ID25, considering the betatron phases between the IDs and the BPM heads. The measured values of the response matrix elements between the selected BPMs and the fast corrector magnets for ID23/25 are listed in Table 1. The periodic COD variations during the kicker operations are measured by using the fast acquisition (FA) mode of the BPM circuit with a sampling rate of 10 kHz. The two trigger signals synchronized with the kicker drivers of THUs, ID23 and ID25, are fed to a digitizer board on the common MTCA.4 system for the BPM23-2 and 24-5. The other two BPM data are synchronized with the kickers by marking with the common timestamps of the fed trigger signals which are shared on the control network of the accelerator. The correction patterns are updated by adding the counter-kick patterns calculated from the 4-BPM data to the previous patterns.

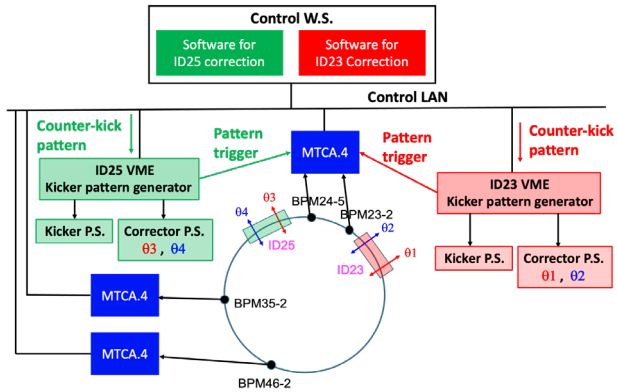

Figure 3: Overall picture of the adaptive feedforward control system at SPring-8.

Table 1: Measured 4-by-4 Horizontal Response Matrix

R_{ij} (m/rad)	ID23-U (θ_1)	ID23-D (θ_2)	ID25-U (θ_3)	ID25-D (θ_4)
BPM23-2 (x_1)	+26.4	+25.6	-3.07	+1.05
BPM24-5 (x_2)	+0.623	-3.29	+25.6	+25.8
BPM35-2 (x_3)	-2.08	+1.66	-22.8	-20.2
BPM46-2 (x_4)	-18.2	-20.9	+6.69	+2.71

Folding and Filtering Processes of BPM Data

To achieve orbit correction accuracy of less than 1 μm (rms), the counter-kick errors of the fast correctors need to be within 0.05 μrad (rms). The keys of BPM data processing are random noise reduction to secure sub-micron resolution and filtering to eliminate contamination due to error kicks other than the THUs. For low-noise extraction of the periodic COD variation, the BPM data of several tens of periods in length is folded at the period of the helicity switching. In the case of helicity switching at 1 Hz, for example, the BPM data sampled at 10 kHz of 60 periods in length is firstly fast-Fourier-transformed (FFT) in the frequency range from –5 kHz to +5 kHz. We then pick up every peak accurately at the repetition frequency of the switching kicker and its harmonic frequencies by spline interpolation of the FFT spectrum. Inverse Fourier transform of the data picked-up at the fundamental and harmonic frequencies yields the time profile of periodic orbit variation folded at the period of the helicity switching. In the case of helicity switching at 0.1 Hz, the BPM data of 10 periods in length is folded by a similar procedure. For high frequency noise reduction, the 5-th orders Butterworth numerical low-pass filter is applied to the data in the frequency domain before the inverse Fourier transform. The filter cut-off frequency is 100 Hz and 30 Hz for switching at 1 Hz and 0.1 Hz, respectively. To accurately counteract error sources, it is important to compensate time response (phase delay) of the AFC correction loop itself. The phase delay in the frequency domain was derived from a step response of the BPMs measured by exciting the correctors with a step function. The phase delay compensation was incorporated into a phase function of the complex low-pass filter.

ISBN: 978-3-95450-241-7 ISSN: 2673-5350 doi:10.18429/JACoW-IBIC2022-WE2I3

By this folding and filtering processes of raw BPM data, we can obtain an averaged and smoothed one-cycle time profile of the periodic orbit variation at the switching frequency. After the folding and the filtering, the random noise level of the BPM data is 0.2 μm (rms).

Counter Kick Calculation

In our AFC system, counter-kick patterns for the four corrector magnets in the two THUs are calculated using the processed four BPMs data by solving Eq.(1) with the singular value decomposition (SVD) method. The 4-by-4 response matrix elements R_{ij} between the BPMs and the correctors are measured as shown in Table 1. In the case of the simultaneous helicity switching of ID23 and ID25, the corresponding singular values of the 4-by-4 response matrix are shown in Table 2, in descending order from four modes #1 to #4. Solving Eq.(1) with the SVD using all the four modes is equivalent to simply multiplying the inverse of the response matrix. Calculated CODs (RMS of values at the four BPMs) corresponding to each mode excited by a random kick of 0.1 μrad (1σ) at each corrector magnet are shown in Table 2. The CODs of modes #1 and #2 are the main components of the orbit variation and are larger than that of the modes #3 and #4. The CODs of modes #1 and #2 apparently need to be corrected. Modes #3 and #4 have significantly smaller contributions to the orbit variation. However, solving by using only two modes of #1 and #2 resulted in calculated counter-kicks with an inappropriate kick angle and sign. Comparing the BPM noise-derived errors of the counter-kicks between "3-mode case" correcting modes #1 through #3 except mode #4, and "4-mode case" correcting all four modes, the former is 0.05 μrad (1σ) and the latter is 0.1 μrad (1σ), indicating that the "4-mode case" does not satisfy the target correction-kick accuracy of 0.05 μrad (1σ). Therefore, we decided to calculate the counter-kicks in the "3-mode case" (discarding mode #4).

Table2: Singular Values of the 4-by-4 Response Matrix. RMS values of calculated CODs in micron unit at the 4-BPMs corresponding to each mode when the random kick of 0.1 μrad (1σ) is given at each correction kicker.

Mode #	Singular Values	ID23-U kick	ID23-D kick	ID25-U kick	ID25-D kick
1	50.4	0.94	1.2	3.9	1.3
2	43.7	1.3	1.2	0.84	1.0
3	1.89	0.05	0.04	0.05	0.06
4	1.22	0.03	0.04	0.03	0.02

In the case of the solo helicity switching of ID23 or ID25, counter-kick patterns at the two corrector magnets for each of ID23 and ID25 are calculated from the four-BPM data by solving Eq. (1) with SVD using all modes with two singular values of the 4-by-2 response matrix, in other words, multiplying by the pseudo-inverse response matrix. The errors in the solved counter kicks derived from the BPM error of 0.2 μm (1σ) are about 0.03 μrad (1σ) for both ID23 and ID25, which satisfy the target correction kick accuracy.

Experimental Verifications

The new correction scheme based on the AFC was experimentally verified and successful for both solo and simultaneous switching at ID23 and ID25. Here, as an example, a demonstration for simultaneous 1 Hz switching is described. Orbit fluctuations were detected at all the four BPMs with the initial correction patterns in the feedforward correction tables for the two THUs. Following the aforementioned procedure, we obtained the counter-kick data for updating the feedforward correction tables for both IDs. The calculation of counter-kick data for each ID was separately processed by using all the four BPM data synchronized with the respective kicker triggers. The observed periodic orbit variations before and after modifying the correction patterns, along with the frequency-domain orbit fluctuation, are shown in Fig. 4, in which the periodic COD variations folded at the period of the kicker trigger for ID23 are shown. The pole gaps were 20 mm and 60 mm for ID23 and ID25, respectively. After the modification of the feedforward correction pattern, the horizontal COD fluctuations were drastically damped to the background level without helicity switching. We also checked for adverse effects of the horizontal corrections on the vertical COD as that could be induced by, e.g., tilted magnetic field in the fast corrector magnets due to fabrication and installation errors. The horizontal corrections worked well without compromising on the vertical beam stability.

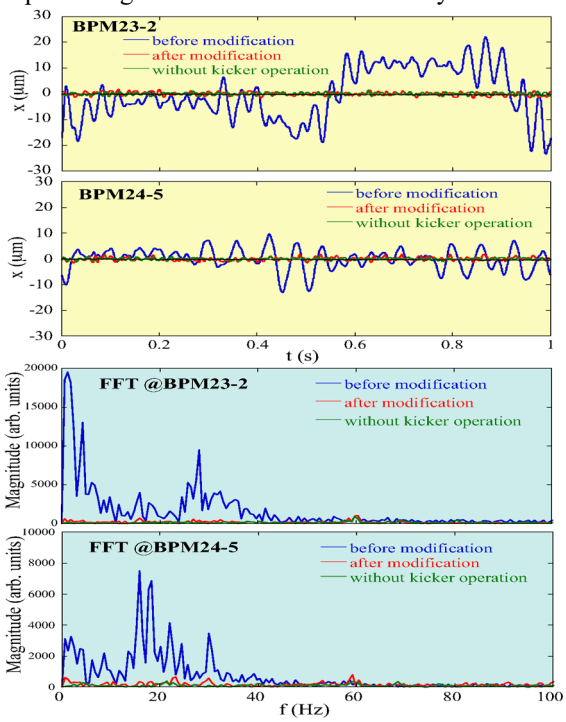

Figure 4: Example of the simultaneous 1 Hz switching of ID23 and ID25. Horizontal orbit fluctuations and their FFT spectra before and after modification of the correction patterns are shown.

Long-term Performance

We applied the developed AFC to the helicity switching of ID23 during the user time operation to confirm its long-

ISBN: 978-3-95450-241-7 ISSN: 2673-5350 doi:10.18429/JACoW-IBIC2022-WE2I3

term performance in suppressing the periodic COD variations. The feedforward correction patterns were automatically updated at 10 minutes intervals at that time. Figure 5 shows the RMS-fluctuation trend of the periodic COD patterns (chosen as an indicator of the magnitude of the periodic orbit fluctuation at 1 Hz) observed by BPM23-2, together with the pole gap of ID23. With the AFC, the orbit variation was successfully suppressed below the target value of 1 μm (rms) over the long period of term. The orbit fluctuation jumped up just after the ID23 pole gap changed, but it was promptly reduced by a subsequent correction by the AFC system.

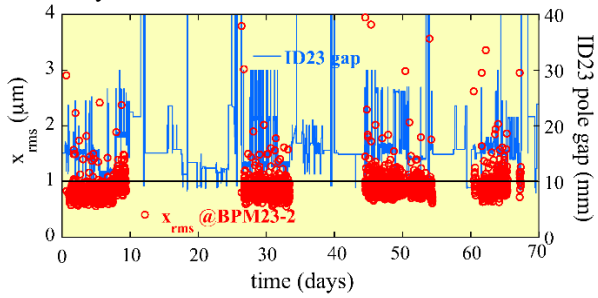

Figure 5: Example of RMS horizontal orbit fluctuation (red dots) with the continuous AFC operation during the ID23 helicity switching. Blue line shows the pole gap of ID23.

WHY NOT USE FAST ORBIT FEEDBACK

Potential Risk of FOFB

Fast orbit feedback (FOFB) is based on a global orbit correction scheme for fast orbit variations. The global correction has the advantage that it can be available in situations where error sources in a ring cannot be identified. However, the correction accuracy is limited by the number and placement of BPMs and correctors. There is a potential risk of unwanted orbit distortions or local bumps, because the correctors are not always placed at the positions or in the vicinity of the error sources.

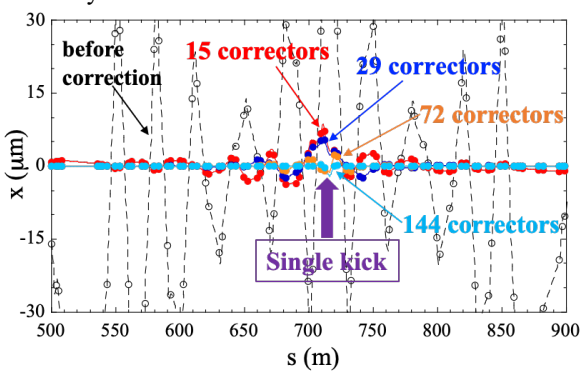

Figure 6: COD correction accuracy depending on the number of correctors with equal spacing, assuming an error source of horizontal single kick of 1 μrad at s=716.05 m. Dots show the horizontal orbits at the BPMs.

We simulated assuming the optics of the SPring-8 storage ring. Simulation conditions are assumed to be as follows: 1) an error source is a horizontal single kick of 1 μrad at s=716.05 m in the ID25 section, 2) numbers of correctors are assumed to be 15, 29, 72, and 144 with equal spacing, and 3) number of BPMs to detect the COD is fixed to be 286 which is all BPMs of the ring. The simulation results in Fig. 6 show that the COD correction accuracy depends on the number of correctors. A small number of the correctors results in unwanted orbit bumps around the error kick. Only the case of 144 correctors shows that such the local orbit bump dose not almost appear, in which the correctors exist within a few meters from the error kick.

Advantage of the AFC

In case that error sources are known, the AFC is much more advantageous than FOFB of the global correction scheme. On the AFC based on a source suppression scheme, the dedicated fewer correctors placed near error sources counteract them efficiently and precisely. A feedforward control such as the AFC is particularly suitable for correcting ID-induced orbit variations. Because we can grasp in advance the characteristics of the error kicks. In an ID section, which is a drift space, at least two correctors up- and down-stream near the error source would be sufficient, not to leak the orbit distortion outside the section. In this case, two counter kicks are approximately allocated in the ratio of the distances from the error kick to each corrector.

CONCLUSION

The development and verification of a new COD correction technique with the adaptive feedforward control (AFC) have been successfully done at SPring-8. The AFC works well for suppressing fast periodic orbit fluctuations during user time operation using the helicity-switching undulators with kickers. It keeps the COD fluctuation suppressed with sub-micron order for a long time.

Toward ultimate photon beam stability for next-generation light sources, relying solely on the global correction scheme, including FOFB, is not sufficient. When the error source is known, for example such as an insertion device origin, a source suppression scheme such as the AFC can be very effective. We believe that the global correction and the source suppression, both of the schemes in a complementary relationship, are indispensable in achieving the ultimate photon beam stability in future light sources.

REFERENCES

[1] T. Hara *et al.*, "Spring-8 twin helical undulator", *J. Synchrotron Radiat.*, vol. 5, pp. 426-427, 1998. doi:10.1107/S0909049597015719

[2] T. Hara *et al.*, "Helicity switching of circularly polarized undulator radiation by ocal orbit bumps", *Nucl. Instrum. Methods Phys. Res., Sect. A*, vol. 498, pp. 496-502, 2003. doi:10.1016/S0168-9002(02)02145-9

[3] M. Masaki *et al.*, "Adaptive feedforward control of closed orbit distortion caused by fast helicity-switching undulators", *J. Synchrotron Radiat.*, vol. 28, pp. 1758-1768, 2021. doi:10.1107/S160057752101047X

[4] H. Maesaka *et al.*, "Development of MTCA.4-Based BPM Electronics for SPring-8 Upgrade", in *Proc. IBIC'19*, Malmö, Sweden, Sep. 2019, pp. 471-474. doi:10.18429/JCoW-IBIC2019-WEBO03